Astron. Astrophys. 360, 1107–1116 (2000)

ASTRONOMY AND ASTROPHYSICS

The stellar content of the compact H II region Sh2-88B⋆,⋆⋆,⋆⋆⋆

L. Deharveng[1], **D. Nadeau**[2], **A. Zavagno**[1], **and J. Caplan**[1]

[1] Observatoire de Marseille, 2 Place Le Verrier, 13248 Marseille Cedex 4, France (deharveng@observatoire.cnrs-mrs.fr)
[2] Observatoire du Mont Mégantic et Département de Physique, Université de Montréal, C.P. 6128, Succ. Centre-ville, Montréal, QC, Canada H3C 3J7 (nadeaud@ere.umontreal.ca)

Received 19 February 2000 / Accepted 19 April 2000

Abstract. We present a photometric study of the compact H II region Sh2-88B and its associated stellar cluster. The positions and *JHK* magnitudes are obtained for 125 stars over an $80'' \times 80''$ field centered on the region.

The region has two components, called Sh2-88B1 and Sh2-88B2. B1 is a compact cometary H II region associated with a cluster containing several massive stars. The dominant exciting star, at the center of the cometary structure, has an ionizing radiation flux corresponding to a spectral type in the range O8.5V–O9.5V. It is highly reddened, with a visual extinction in the 30–42 mag range, and exhibits a near-IR excess. B1 has a simple morphology, with the ionized and neutral gas clearly separated. Its unidentified infrared band (UIB) emission, observed by ISOCAM in the 5–8.5 μm passband, comes from the photodissociation region at the periphery of the ionized gas. B2 is an ultracompact H II region whose exciting star, probably of spectral type later than B0.5V, is not detected; this indicates a visual extinction greater than 60 mag. A very steep and regular increase of the extinction from west to east is observed over the whole of Sh2-88B.

Key words: stars: early-type – stars: formation – ISM: H II regions – ISM: individual objects: Sh2-88B – infrared: stars

1. Introduction

The formation of low and intermediate mass stars involves gravitational collapse and subsequent accretion. This scenario would seem to fail for massive stars: the radiation pressure exerted by a $10\ M_{\odot}$ stellar core on the dust in the infalling gas would halt the accretion, thus limiting the star's mass (Yorke & Krugel 1977). However, this constraint is less restrictive if the accretion is not spherically symmetric but proceeds via a disk (Jijina & Adams 1996; see also Yorke & Welz 1996 for a discussion of the presence of such disks around massive stars).

Near-IR observations show that massive stars are often found at the centers of relatively rich clusters (Testi et al. 1999 and references therein). The best example of clustering around massive stars is that of the Orion Nebula cluster with the Trapezium at the center. Bonnell & Davies (1998) have shown, through numerical simulations, that the central positions of the Trapezium's massive stars cannot be due to dynamical mass segregation; hence these stars must have formed near the cluster center. This situation has prompted new scenarios of massive star formation, involving accretion or collisions at the very center of dense clusters (Bonnell et al. 1998, Stahler et al. 2000).

Both accretion-induced formation and collision-induced formation require that the massive stars form at the center of a populous cluster. Thus massive stars should never form in isolation; those that are found alone must have been ejected from such dense systems. Furthermore, wind-blowing massive stars ejected with high velocities (V$\geq$10 km s^{-1}) form H II regions with a particular long-lasting morphology: cometary compact H II regions with bow shocks (Van Buren et al. 1990, Mac Low et al. 1991), easily identifiable.

The youngest massive stars are found to be associated with ultracompact (UC) and compact H II regions – i.e. H II regions in the first phases of their evolution. The present study of Sh2-88B is part of a larger program aimed at the determination of the stellar content of young H II regions, especially the multiplicity/singularity status of their exciting stars. Sh2-88B contains two components: a compact cometary H II region and a UC H II region. In Sect. 2 we give a brief description of Sh2-88B. In Sect. 3 we present near-IR observations of the region, and we discuss its stellar content in Sect. 4. ISOCAM observations of the emission in the 5–8.5 μm passband, presented in Sect. 5, reveal the distribution of the associated dust. Sect. 6 is devoted to a general discussion of the region (distance, ionization, morphology, clustering of stars, etc.). A comparison of our near-IR photometry with the results of previous studies is given in Appendix A.

Send offprint requests to: L. Deharveng

⋆ Based on observations done at the Canada-France-Hawaii Telescope and at the Observatoire de Haute Provence. The CFHT is operated by the Centre National de la Recherche Scientifique of France, the National Research Council of Canada, and the University of Hawaii.

⋆⋆ Table 1 is available at the CDS via anonymous ftp to cdsarc.u-strasbg.fr (130.79.128.5) or via http://cdsweb.u-strasbg.fr/Abstract.html

⋆⋆⋆ Fig. 3 is only available electronically with the On-Line publication at http://link.springer.de/link/service/00230/

2. Description of the region

The emission nebula Sh2-88B – coincident with the radio source G61.48+0.09 – is a compact object situated 2.4 kpc from the Sun (see Sect. 6.1 for a discussion of the distance). It belongs to a large complex of molecular material, ionized gas, and dust (see Figs. 1 and 2 of Lortet-Zuckerman 1974 for a large-field optical image).

Sh2-88B consists of two regions of ionized gas: an extended cometary source, G61.47+0.09 B1, whose head lies at $\alpha_{1950} = 19^{\rm h}44^{\rm m}42\overset{\rm s}{.}7$, $\delta_{1950} = +25°05'21''$, and a UC source, G61.47+0.09 B2, at $\alpha_{1950} = 19^{\rm h}44^{\rm m}43\overset{\rm s}{.}4$, $\delta_{1950} = +25°05'20''$ (Felli & Harten 1981, Garay et al. 1993, Garay et al. 1994). In the following we call these sources B1 and B2. B1 is partially visible in the optical range, but B2 has no optical counterpart. As shown by Fig. 1, the Hα brightness decreases very sharply towards the peak of the B1 radio structure, suggesting that the head of this cometary source is deeply embedded within a molecular cloud (Pipher et al. 1977, Deharveng & Maucherat 1978, Felli & Harten 1981, Evans et al. 1981, Garay et al. 1994).

This molecular cloud has been mapped in CO by White & Fridlund (1992), who estimate its mass to be $\geq 1000\ M_\odot$ ($\sim$5200 $M_\odot$ for Goetz et al. 1999). The core of the cloud ($\sim$400 $M_\odot$) is a horseshoe-like structure which surrounds the H II region. A very sharp cutoff in the CO emission is observed at the inner edge of this structure, coinciding with the sharp northeast limit of the optical nebula (Fig. 1).

Phillips & Mampaso (1991) have detected and mapped a bipolar CO outflow, whose center (near $\alpha_{1950} = 19^{\rm h}44^{\rm m}42\overset{\rm s}{.}5$, $\delta_{1950} = +25°06'$) lies outside the field studied in this paper. However, as stressed by White & Fridlund (1992), the small scale structure of the molecular cloud is complex, with many substructures at different velocities, and "it is possible that one or several more outflows" are present, but "more sensitive observations are needed to clarify this issue".

H_2O maser emission has been reported by Blair et al. (1978) and by Henkel et al. (1986) (at $\alpha_{1950} = 19^{\rm h}44^{\rm m}42\overset{\rm s}{.}0$, $\delta_{1950} = +25°05'30''$). This source may be highly variable, subsequent observations having failed to detect it (Wouterloot et al. 1993, Comoretto et al. 1990).

Sh2-88B is associated with the infrared source IRAS 19447+2505, whose luminosity Chini et al. (1986) estimate to be 1.47 10^5 $L_\odot$ (corrected for a distance of 2.4 kpc). In the near-IR, the K' frame of Hodapp (1994) shows a stellar cluster associated with extended nebulosity. This cluster is the object of the present study.

3. Near-IR observations

We observed Sh2-88B in the near IR at the 3.6-m Canada-France-Hawaii telescope on the night of 1996 July 1, using MONICA – the Montreal IR camera (Nadeau et al. 1994). Frames were obtained through the J, H, and K broad-band filters with total integration times of 720 s, 160 s, and 100 s respectively. Details about the instrumentation and the calibration can be found in Deharveng et al. (1999).

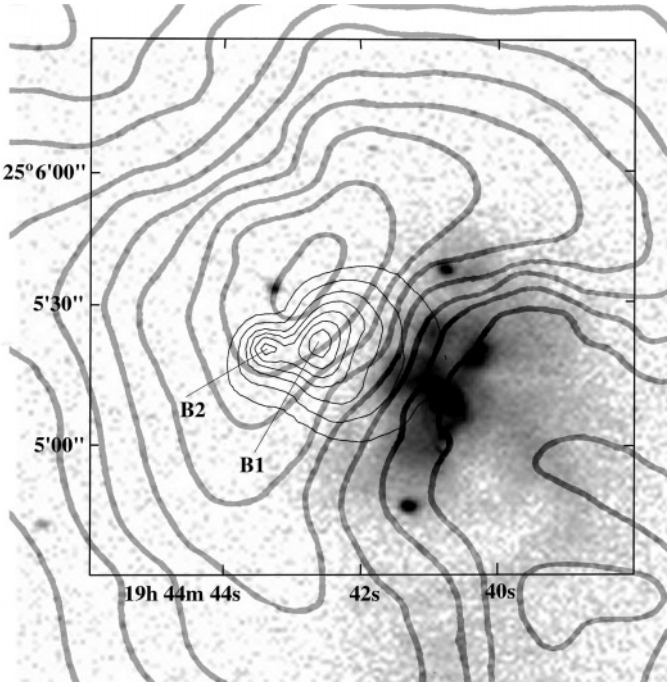

Fig. 1. CO emission (thick grey lines) and radio continuum emission (thin black lines) superimposed on an Hα frame of the Sh2-88B region (B1950 coordinates). The CO $J = 2$–1 emission is from White & Fridlund (1992); in this map the antenna temperature is integrated over a velocity channel of 1 km s^{-1} centered at 22 km s^{-1} – the velocity of the ionized gas at the head of the cometary B1 structure. The radio continuum emission at 8.3 GHz is from Garay et al. (1998b). The Hα frame was obtained at the Observatoire de Haute Provence with the 120-cm telescope. North is up and east is left. The size of the field is $2\overset{'}{.}1 \times 1\overset{'}{.}8$.

The frames were reduced using the DAOPHOT stellar photometry package (Stetson 1987), with PSF fitting. As all the frames exhibit a non-uniform nebular background which hampers accurate photometry, the iterative procedure described in Deharveng et al. (1992) was used. The error estimates given by DAOPHOT do not take into account the additional uncertainty due to the somewhat subjective decisions necessary when stars are superimposed on a bright, highly variable background. To estimate the errors more realistically, we have compared the magnitudes obtained from independent reductions performed by two different people. The difference between the results is smaller than 0.1 mag for the bright stars, but can reach 0.3 mag for stars near the detection limit.

The right ascensions and declinations were obtained from the frame coordinates given by DAOPHOT, using a linear transformation determined from four stars in common with the USNO-A1.0 catalog. Subsequently the A2.0 version of this catalog appeared (Monet et al. 1998), with all the stars in this area of the sky systematically shifted because of the change of reference frame; we therefore applied this shift to our stars. The final positional uncertainty, probably well under $1''$, is dominated by detector distortion.

Table 1. Coordinates and *JHK* photometry of all the stars in an $80'' \times 80''$ field centered on Sh2-88B. This table is available only in electronic form.[2]

Table 2. Coordinates and photometry of the stars mentioned in the text. The numbers in parentheses correspond to the Goetz et al. (1999) identification.

No.	RA (B1950)	Dec (B1950)	K	$J-K$	$H-K$	A_V
13	$19^h\ 44^m\ 43\overset{s}{.}38$	$+25^\circ\ 04'\ 41\overset{''}{.}1$	12.27	+3.55	+1.28	21.0
19 (3)	$19^h\ 44^m\ 41\overset{s}{.}20$	$+25^\circ\ 04'\ 47\overset{''}{.}6$	9.50	+0.92	+0.22	6.0
23 (13)	$19^h\ 44^m\ 42\overset{s}{.}09$	$+25^\circ\ 04'\ 48\overset{''}{.}9$	13.22	+1.92	+0.62	11.1
42 (15)	$19^h\ 44^m\ 40\overset{s}{.}38$	$+25^\circ\ 04'\ 59\overset{''}{.}6$	13.31	+1.76	+0.40	10.2
50	$19^h\ 44^m\ 42\overset{s}{.}10$	$+25^\circ\ 05'\ 04\overset{''}{.}2$	12.69	+3.90	+1.72	23.0:
56 (17)	$19^h\ 44^m\ 40\overset{s}{.}90$	$+25^\circ\ 05'\ 05\overset{''}{.}8$	12.59	+2.45	+0.82	14.5
61 (19)	$19^h\ 44^m\ 41\overset{s}{.}40$	$+25^\circ\ 05'\ 08\overset{''}{.}2$	12.24	+2.48	+0.89	14.7
82 (7)	$19^h\ 44^m\ 41\overset{s}{.}88$	$+25^\circ\ 05'\ 19\overset{''}{.}7$	9.48	+7.14	+3.08	30–42:
83 (24)	$19^h\ 44^m\ 41\overset{s}{.}60$	$+25^\circ\ 05'\ 19\overset{''}{.}8$	11.00	+2.43	+0.88	14.7
84 (25)	$19^h\ 44^m\ 41\overset{s}{.}33$	$+25^\circ\ 05'\ 20\overset{''}{.}0$	12.52	+1.99	+0.71	11.6
111	$19^h\ 44^m\ 41\overset{s}{.}57$	$+25^\circ\ 05'\ 34\overset{''}{.}0$	12.00	+4.08	+1.71	24.2:
112 (30)	$19^h\ 44^m\ 43\overset{s}{.}33$	$+25^\circ\ 05'\ 34\overset{''}{.}6$	11.29	+0.83	+0.16	5.4
116	$19^h\ 44^m\ 42\overset{s}{.}62$	$+25^\circ\ 05'\ 36\overset{''}{.}9$	12.65	+5.74	+2.46	34.0:
119 (1)	$19^h\ 44^m\ 40\overset{s}{.}58$	$+25^\circ\ 05'\ 38\overset{''}{.}5$	9.79	+0.77	+0.44	5.2

4. Results

In this paper all the J, H, and K magnitudes are given after transformation to the UKIRT system.

Table 1 gives the B1950 coordinates[1], J, $J-H$, and $H-K$ magnitudes and colors obtained for 125 stars in the $80''\times80''$ field centered on Sh2-88B; 64 stars are detected in all three bands. The faintest stars we detect are of approximate magnitudes 19.5 in J, 17 in H, and 16 in K; however the sample is not complete up to these limits, the faintest stars being more difficult to detect if superimposed on a bright non-uniform nebulosity.

Table 1 is available only in electronic form[2]. Table 2, which is extracted from Table 1, includes all the stars discussed in the text.

4.1. Images

Fig. 2 shows the J, H, and K frames. These frames are displayed with logarithmic scales in order to enhance the low brightness stars and the background nebulosity. The stars discussed in the text are identified on the H frame by the same numbers as in Tables 1 and 2.

Fig. 3 is a color composite image of the region. This image mostly shows the effects of extinction, the color differences of the stars being due mainly to differences in reddening and only slightly to differences in intrinsic color (we show in Sect. 4.2 that very large extinction variations are observed from star to star).

A reflection nebulosity covers almost all of the field, especially west and south. A dark absorbing cloud lies in the center. This dark cloud is very inhomogeneous. The contrast between the bright and the dark zones is highest in the K band. On the color image the reflection nebula appears blue in the western and southern parts of the field, and red at the edges of the central absorption cloud.

The brightnesses of the stars differ considerably between J and K. We call attention to the three central stars, numbers 82, 83, and 84, which are situated in a region of highly variable extinction, at the eastern edge of the optical H II region, and at the western edge of the central absorbing cloud. Star 82, which is faint in J, is the brightest star of the field in K. It appears red in the color image. As discussed in Sect. 4.2, star 82 is most probably the exciting source of the B1 H II region.

Fig. 4 shows the radio continuum emission, as observed at 8.3 GHz by Garay et al. (1998a), superimposed on the K frame. The radio continuum shows the bright head (invisible at optical wavelengths) of the cometary H II region B1, along with the UC H II region B2, in the direction of the central absorbing cloud. Star 82 lies at the center of the cometary structure. Note the remarkable alignment of star 84, star 83, star 82, the core of B1, and finally B2.

4.2. Color-magnitude and color-color diagrams

Fig. 5 shows the K versus $(J-K)$ diagram. We have drawn the main sequence assuming a distance of 2.4 kpc (Sect. 6.1) and no

[1] The reference coordinates are in the J2000 system, but for convenience of comparison with published radio data we give the B1950 positions of our stars, based on the transformation from J2000 outlined in the Astronomical Ephemeris and assuming zero proper motions, radial velocity, and parallax in the J2000 system. Within our small field the J2000 coordinates can be retrieved to within $0\overset{''}{.}4$ by adding $+2^m05\overset{s}{.}69$, $+7'\ 26\overset{''}{.}1$.

[2] Table 1 is available at the CDS (via anonymous ftp to cdsarc.u-strasbg.fr or via http://cdsweb.u-strasbg.fr/Abstract.html) as well as at http://www-obs.cnrs-mrs.fr/matiere/Sh2-88B/Table1.html

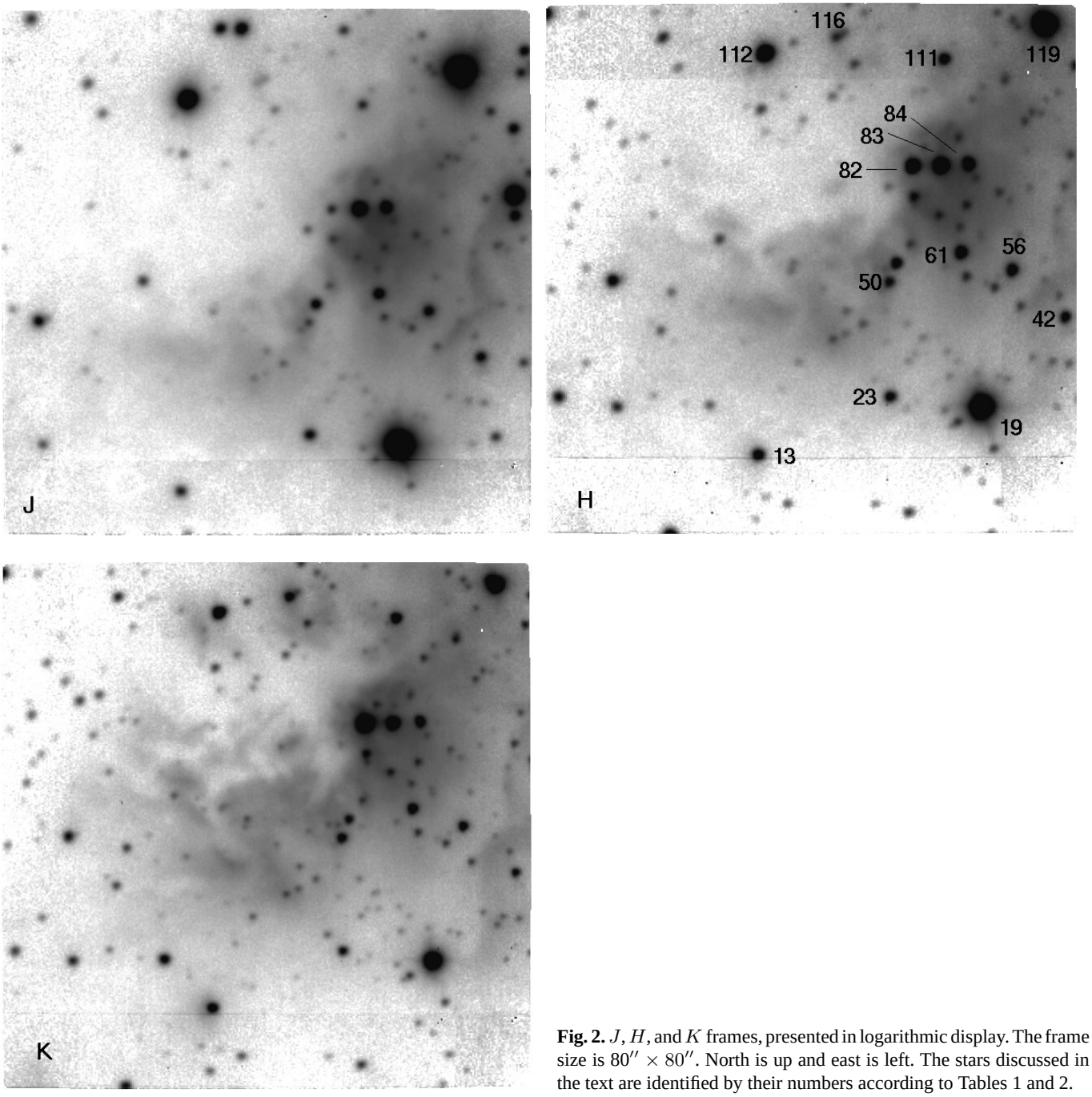

Fig. 2. J, H, and K frames, presented in logarithmic display. The frame size is $80'' \times 80''$. North is up and east is left. The stars discussed in the text are identified by their numbers according to Tables 1 and 2.

Fig. 3. Color composite of the images in Fig. 2 (blue for J, green for H and red for K). This figure is not available in the printed publication but is available in the on-line version (http://link.springer.de) and also can be found on the Web at http://www-obs.cnrs-mrs.fr/matiere/Sh2-88B/JHK.jpg

extinction. We have also drawn the interstellar reddening lines (according to Mathis 1990, with $R_V = 3.1$) originating from an O9V star (a likely spectral type for the exciting star of B1; see Sect. 6.2) and a B2V star; their lengths correspond to $A_V = 40$ mag. In Table 2 we give an estimate of the extinction, obtained from this color-magnitude diagram, assuming that all the objects are main-sequence stars. Of course this estimate is quite uncertain; not only may the extinction differ from the standard law, but several of the objects may present some infrared excess.

Three bright stars – numbers 19, 112, and 119 – are affected by a relatively small 5–6 mag of visual extinction. This is somewhat more than one would expect from the general interstellar extinction over a distance of 2.4 kpc; thus these stars are probably associated with the complex, but located in front of the core. Star 82 is the brightest and (of those stars measured in all three bands) the most reddened star of the field. The extinction varies

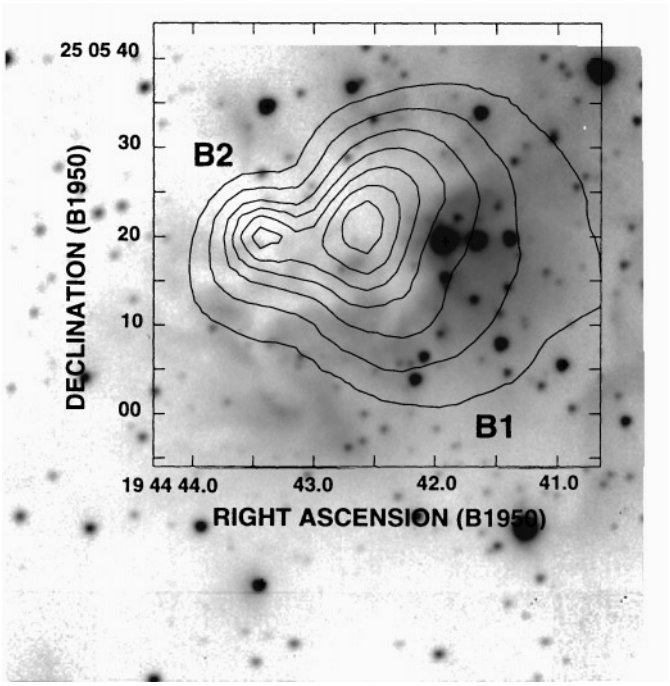

Fig. 4. Radio continuum emission at 8.3 GHz (Garay et al. 1998a) superimposed on the K frame of Sh2-88B.

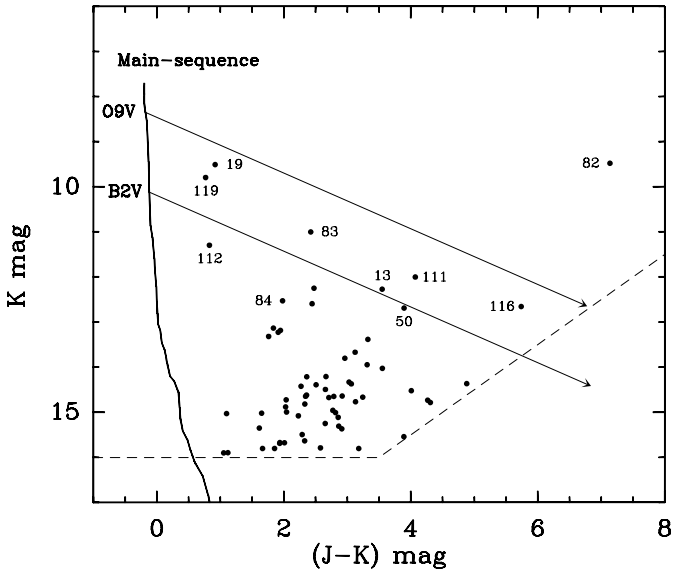

Fig. 5. The K versus $(J-K)$ magnitude-color diagram. The main sequence is from Vacca et al. (1996) for O stars and from Schmidt-Kaler (1982) for later spectral types. Reddening lines are drawn originating from O9V and B2V stars; they correspond to a visual extinction of 40 mag, for the standard interstellar reddening law of Mathis (1990) with $R_V = 3.1$. The dashed lines show our detection limits.

considerably in its vicinity; it increases from west to east, from stars 84 to 83 to 82. Star 82 is most probably the exciting star of B1, both on the basis of its position – at the center of the cometary structure – and on the basis of its high luminosity. A number of bright reddened stars – 13, 83, 111, and 116 – may participate in the ionization of this H II region.

Fig. 6 shows the $(J-H)$ versus $(H-K)$ diagram. Again the main-sequence and the reddening lines – for $A_V = 40$ mag – are plotted. Most of the stars appear to be reddened main- sequence stars. The extinctions estimated from this diagram agree with those estimated from K versus $J-K$ in Fig. 5. No object with an apparently strong near-IR excess is observed. The near-IR colors of star 82 indicate a visual extinction of about 42 mag, and a very small IR excess. But according to Fig. 5, star 82 is clearly overluminous for a main-sequence OB star. The origin of this overluminosity is discussed in Sect. 6.3.

B2 lies in the direction of the central absorbing cloud. No conspicuous reddened star is detected in this direction. If the exciting star of B2 is of spectral type B1V, its non-detection up to a K magnitude of 16 indicates a visual extinction $\geq$61 mag. Thus the extinction continues to increase eastward of star 82.

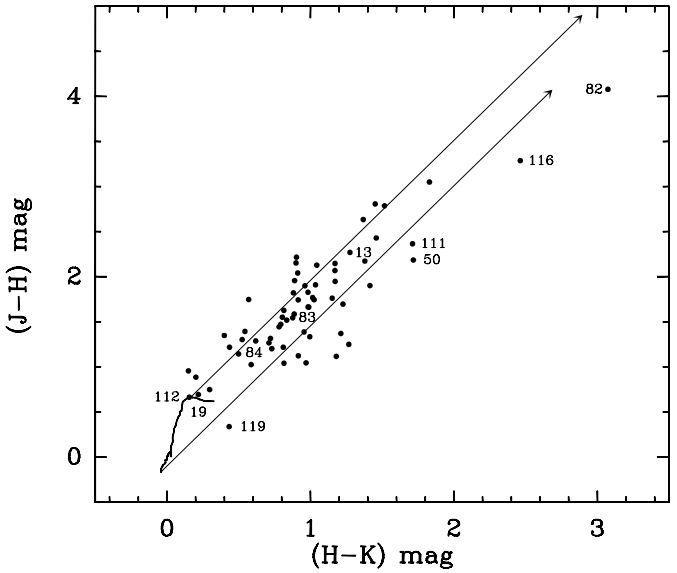

Fig. 6. The $(J-H)$ versus $(H-K)$ color-color diagram. The main-sequence and the reddening lines corresponding to a visual extinction of 40 mag are shown as in Fig. 5.

4.3. A trapezium system

Massive stars are often found associated with dense clusters containing low mass stars as well. This is the case of Sh2-88B1. The system of massive stars associated with B1, although composed of three aligned stars, is an example of a "trapezium system" as defined by Allen et al. (1977); it contains at least three massive stars (82, 83, and 84) whose relative separations within the system do not exceed a factor of three; the maximum separation of the three components (in the plane of the sky) is 18 000 AU. Similar separations are found in the young trapezium systems associated with the compact H II region Sh 138 (Deharveng et al. 1999) and with AFGL 437 (in preparation). For comparison, the Trapezium in the Orion Nebula has an O6 primary component and a maximum separation of 10 000 AU.

5. ISOCAM observations

In order to study Sh2-88B's dust content, we have observed it with ISOCAM (cf. Cesarsky et al. 1996), the camera on board the Infrared Space Observatory (ISO). The observation was made in the beam- switching mode on 1998 March 29, during revolution 602. The pixel size was $3''.0$ square. The LW2 filter (5–8.5 μm) was used to observe the dust emission, mainly the unidentified infrared bands centered at 6.2 and 7.7 μm. The data were analyzed using the CIA package (Ott et al. 1997) version 3, following the classical procedure (Stark et al. 1999): dark correction, deglitching, stabilization, and calibration as described in Zavagno & Ducci (2000).

A point-like source is observed on the original LW2 map, $6''$ north of star 82. The observed flux density of this source is 0.73 Jy ($\pm 10\%$); this agrees with the extrapolation to 6.75 μm of the *JHK* magnitudes of star 82. We assume that this point source corresponds to star 82 and have shifted the original ISOCAM map to make the source coincide with our measured position of the star. According to A. Abergel (private communication), some ISOCAM coordinates may have errors of this order. The resulting map is presented in Fig. 7a. Fig. 7b shows a 6 cm VLA map of the region, kindly provided by G. Garay, superimposed on the LW2 emission.

The area covered by the ISOCAM field – almost the whole Sh2-88B region – has an observed flux density in the LW2 filter of 130 Jy. This agrees with the spectral energy distribution presented by Evans et al. (1981; their Fig. 6).

The LW2 emission is probably dominated by the 6.2 and 7.7 μm unidentified infrared bands (UIBs). These bands, together with those centered at 3.3, 8.6, and 11.3 μm, are observed in a great variety of sources and are commonly attributed to large molecules – polycyclic aromatic hydrocarbon (PAH) – or small carbonaceous grains (Léger & Puget 1984, Papoular 1999 and references therein).

The most striking features of the LW2 emission, and thus of the dust distribution, are the following:

- An emission "hole" (zone a in Fig. 7a) is observed towards the ionized region B1.
- The strongest emission is observed at the periphery of B1 (emission peaks b and d in Fig. 7a). Peak c, southwest of B1, is adjacent to an area of increased radio brightness.
- Another emission hole (zone e in Fig. 7a) is observed at the periphery of B1 and B2, between peaks b and d.

Obviously the UIB carriers are absent or strongly depleted in the ionized gas; the highest dust emission is observed at the periphery of the ionized zone, in the direction of the photodissociation region (PDR), as previously observed for dust emission associated with compact H II regions (Zavagno & Ducci 2000). There are several possible reasons for this: i) the UIB carriers are destroyed in the ionized gas; ii) the UIB carriers are excited only in the PDR (e.g. excitation of the functional groups at the grain surface by ambient H^0, as proposed by Papoular 1999); and iii) the anisotropic radiation has driven the grains through the gas, leading to an increase of the dust-to-gas ratio in the PDR, as proposed by Weingartner & Draine (1998). Our unique ISOCAM observation does not allow us to choose among these possibilities.

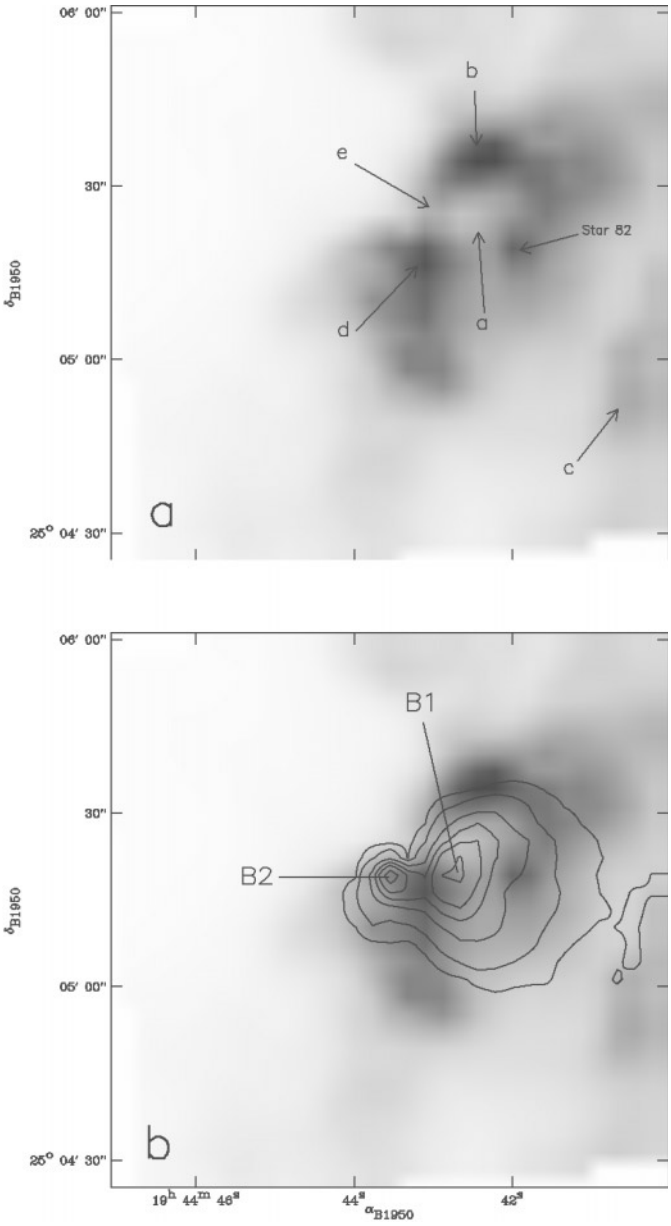

Fig. 7. a LW2 (5–8.5 μm) emission of the Sh2-88B region observed with ISOCAM. Star 82 and the zones discussed in the text are identified. **b** VLA map of 6 cm emission, superimposed on the LW2 emission.

The 3.3 μm emission has been observed in Sh2-88B by Goetz et al. (1998). The 3.3 μm and LW2 emissions are very similar, both emanating from the periphery of the ionized zones; this suggests a common origin. However there is one difference – at the LW2 peak d, where no strong 3.3 μm emission occurs. The 3.3 μm emission peaks south of d – even farther from e. We interpret both the dust emission hole in direction e and the offset between the LW2 and 3.3 μm emission peaks in the nearby direction d as due to high extinction and corresponding reddening by a foreground clump. Since e is close to B2, it is likely that

the same clump is also responsible for the high extinction of B2. This clump lies in front of the PDR of B1.

6. Discussion and conclusions

6.1. The distance of Sh2-88B

Different authors give quite different distance estimates for Sh2-88B. These estimates cluster around two mutually exclusive values: 2.0 kpc (Felli & Harten 1981) and 5.4 kpc (Churchwell et al. 1990, and all the papers by Garay and co-workers). In the following we rediscuss the distance indicators.

A kinematic distance can be derived from the radial velocity of the associated molecular cloud ($V_{\rm LSR}({\rm CO}) = 22.9$ km s^{-1}, Blair et al. 1975 and Blitz et al. 1982; $V_{\rm LSR}({\rm CO}) = 22\pm1$ km s^{-1}, White & Fridlund 1992; $V_{\rm LSR}({\rm NH_3}) = 21.4$–22.3 km s^{-1}, Zinchenko et al. 1997, Churchwell et al. 1990; $V_{\rm LSR}({\rm HCO^+} = 22.8$ km s^{-1}, Pirogov et al. 1995) by using the Galactic rotation curve of Brand & Blitz (1993) with the standard values for the Galactocentric distance of the Sun, 8.5 kpc, and the LSR's circular velocity, 220 km s^{-1}. Two distances, 2.1$\pm$0.2 kpc and 6.0$\pm$0.2 kpc, are possible.

A photometric distance can be derived from the stars LSII+25°09, the exciting star of Sh2-88 A, and LSII+25°08 (HD 338916) the main exciting star of Sh2-88. With a spectral type of B0.5V and UBV photometry from Crampton et al. (1978), LSII+25°09 has a photometric distance of 2.7 or 2.1 kpc, estimated using the absolute M_V calibrations of Vacca et al. (1996) or that of Schmidt-Kaler (1982), respectively. With a spectral type O7V (Avedisova & Kondratenko 1984) and photometry from Hiltner & Iriarte (1955), LSII+25°08 has a photometric distance of 2.6 or 3.0 kpc with the above calibrations. These photometric distances are in good agreement with the near kinematic distance. Another argument in favor of the near distance is given by the OH absorption line near 1665 MHz. This line is observed (Wouterloot et al. 1993) at $V_{\rm LSR} = 21.5$ km s^{-1}, very close to that of the Sh2-88B complex. If this complex were situated at the far distance, the OH absorption due to gas situated between 2.1 kpc and 6.0 kpc would show higher velocities – up to about 32 km s^{-1}. This is not observed.

In the following we adopt a distance of 2.4 kpc for the whole complex.

6.2. The ionization of Sh2-88B

Sh2-88B is a thermal radio continuum source (Felli & Harten 1981, Garay et al. 1994). Its radio flux density allows us to determine $N_{\rm Lyc}$, the number of ionizing photons emitted per second, and hence the spectral type of its exciting star – assuming that a single main-sequence star dominates the ionization. The radio flux densities of sources B1 and B2, measured at 5 GHz by Felli & Harten, are 6.1 Jy and 250 mJy respectively; measured by Garay et al. (1993) they are 4.36 Jy and 830 mJy respectively. We have used Eq. (1) of Simpson & Rubin (1990) to determine $N_{\rm Lyc}$ assuming a distance of 2.4 kpc, ionic abundances He$^+$/H$^+$ of 0.08 for B1 and 0.02 for B2 (Garay et al. 1998b), and an electron temperature of 8000 K (deduced from the temperature- Galactocentric distance relation established for compact and UC H II regions by Afflerbach et al. 1996). Depending on the flux used we obtain $\log(N_{\rm Lyc}) = 48.32$ or 48.52 for B1, and 47.1 or 47.6 for B2. Depending on whether we adopt the absolute M_V calibrations of Vacca et al. (1996) or of Schaerer & de Koter (1997), we obtain for the assumed single exciting star a spectral type of O8.5V or O9.5V for the B1 region and in any case later than B0.5V for the B2 region. Assuming a distance of 5.4 kpc, Garay et al. (1994) obtained spectral types O6V and O8V for the same sources, respectively.

The spectral types we obtain are consistent with the following facts:

- Almost no ionized helium is observed in B2 (Garay et al. 1998b); this would not be the case if the exciting star were an O8V – cf. the photoionization models of Stasińska & Schaerer (1997 – their Fig. 2). This points to a star cooler than B0.5V
- In B1, He$^+$/H$^+$ varies from 0.08 in the central region to 0.06 in the optical outer parts (Deharveng et al. 2000), showing the presence of neutral helium; but all the helium would be ionized with an O6V exciting star (Stasińska & Schaerer 1997).
- The O^{++}/O ionic abundance measured for Sh2-88B1 (Deharveng et al. 2000) is low; once again, this agrees better with an O9V exciting star than with an O6V.

The consistency of these results is a strong corroboration of our choice of the nearer of the kinematic distances.

6.3. The luminosity of star 82

Star 82's IR colors in Fig. 6 seem to indicate a visual extinction of 42 mag, and no conspicuous near-IR excess. But then Fig. 5 shows that, for an O8.5V–O9.5V star, star 82 is some three magnitudes *overluminous* in K and (since the colors are normal) in H and J as well. An error in the H or K measurement cannot explain this overluminosity, as Goetz et al.'s (1999) H and K measurements differs from ours by only 0.05 and 0.22 mag. An incorrect choice of the distance cannot be responsible: if star 82 is an O6V situated at 5.4 kpc as proposed by Garay et al. (1994), then it is 4.5 mag overluminous.

The situation is explained in Fig. 8, showing the spectral energy distributions (based on J, H, and K) of star 82 and of a standard O9V star at 2.4 kpc, as affected by visual extinctions of zero, 30, and 42 mag. With $A_V = 42$ mag, the spectral energy distribution of the reddened O9V star is parallel to that of star 82, but star 82 is *overluminous* by some 3 mag in all three bands. But: star 82 cannot be a supergiant because its ionizing radiation would not be hard enough to account for the degree of excitation of the ionized gas. However, with an assumed A_V of only 30 mag we reproduce the observed J, leaving excess luminosity in H and K. If the fluxes shortward of J are normal (something we cannot verify), then this rise in luminosity from zero in J to about 1.5 mag at H and about 3 mag at K can be described as an IR excess, due perhaps to an accreting envelope or disk. Such an IR excess is not detectable from the $J-H$ vs. $H-K$ diagram because star 82 stays on the reddening line. It is

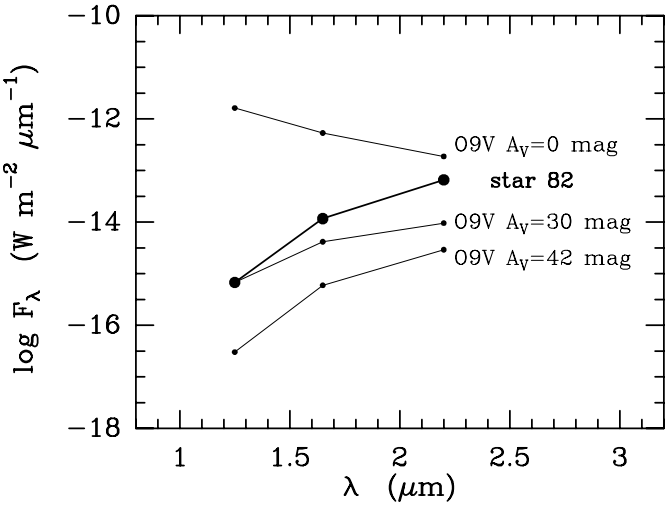

Fig. 8. The spectral energy distributions (based on J, H, and K) of star 82 and of a standard O9V star at 2.4 kpc, as affected by visual extinctions of zero, 30, and 42 mag.

also possible that A_V is somewhat greater than 30 mag (but less than 42 mag), if the IR excess begins before the J band. Thus our conclusion is that the main exciting star of B1, star 82, has a near-IR excess and a visual extinction in the range 30–42 mag (assuming a standard extinction law).

This result is important, as very few O–B2 stars are known to display a near-IR excess. The origin of the excess emission – whether it is produced in a circumstellar disk and/or in an envelope – is unknown in the present case. Star 82 is a possible illustration of the accretion models of Beech & Mitalas (1994) and Bernasconi & Maeder (1996), in which massive stars grow in mass while in their H- burning phase, and evolve up the main sequence while hidden in their optically-thick parental cocoons. Such objects should show IR excesses due to their dusty circumstellar surroundings.

The compact H II region Sh 269 harbors a very similar object – the massive double star IRS2 – which participates in its ionization (Eiroa et al. 1994). IRS2west, with a luminosity of $7.1 \times 10^4 L_\odot$, is the reddest object of the Sh 269 cluster, and is very similar to star 82 both in K magnitude and in the near-IR colors. It is the source of a Herbig-Haro object (Heydari et al. 1982, Eiroa et al. 1994), and thus possibly possesses an accretion disk. (Ejection of matter is generally associated with an accreting disk – cf. the discussion in Königl 1999.) The main exciting star of the compact H II region Sh 138 has also been found to be overluminous, to a lesser degree, in J, H, and K (Deharveng et al. 1999). The exciting star of the compact H II region Sh 266, the Herbig Ae/Be star MWC 137, displays an IR excess (Pezzuto et al. 1997) and emits a very strong ionized wind.

6.4. The extinction of Sh2-88B

We observe over the Sh2-88B region a strong gradient of extinction which is closely correlated with a strong gradient of the CO column density (Fig. 1). The extinction component of general interstellar origin can be estimated from two concordant measurements: i) the minimum stellar A_V – assumed to be due to foreground dust – is in the range 5–6 mag; and ii) the Balmer decrement of the visible H II region, Hα /Hβ = 18.7, corresponds to a visual extinction A_V of 5.5 mag (Deharveng et al. 2000). Thus we assume that any extinction beyond 5.5 mag in V is of local origin. The extinction rises very rapidly from west to east; for example, between stars 84 and 82 we observe an 18–30 mag increase in visual extinction over a distance of 0.1 pc. The extinction continues to rise eastward of star 82, and reaches values $\geq$61 mag in the direction of B2, at the center of the dark cloud. Goetz et al. (1999) present a map of the visual extinction over the whole H II region, obtained from a comparison between the Brγ emission and the 5 GHz radio continuum emission of the ionized gas. We agree with their overall picture: high visual extinction – as high as 70 mag – in the direction of B2, and a regular decrease of the extinction toward the west. But they obtain higher values than we do in the directions of star 82 and of the optical nebula; we believe that these higher values are not real and may be due to a problem of zero level in the calibration of their Brγ image.

6.5. Conclusions

Sh2-88B definitely lies at a distance of about 2.4 kpc, much closer than previously assumed by some authors. The radio continuum flux density, for this distance, indicates a spectral type in the range O8.5V–O9.5V for the exciting star of B1 and later than B0.5V for B2, in good agreement with the observed degree of excitation of the ionized gas.

The main exciting star of B1 has been identified as star 82, which is clearly overluminous in K by some 3 mag with respect to its probable spectral type. This cannot be due to an error in the assumed distance or in the assumed spectral type. We propose that it is indicative of a near-IR excess, possibly due to the presence of an accreting envelope or disk.

The foreground interstellar extinction in the direction of Sh2-88B is ~ 5.5 mag. Furthermore, the whole region shows a regular gradient in extinction, larger than 49 mag over 0.33 pc, from east to west, correlated with the gradient in column density of the molecular material. The highest extinction, $\geq$ 60 mag, is observed in the direction of B2.

The geometry of the cometary source B1 is simple, with the ionized and neutral material clearly separated. Our ISOCAM observation shows that the 6.2 μm and 7.7 μm UIB emission comes from the periphery of the ionized zone, most probably from the PDR. The dense absorbing clump, responsible for the B2 extinction, lies in front of the PDR of B1.

Sh2-88B shows another example of a massive OB star not found in isolation, but associated with a cluster.

The whole region presents a case of sequential star formation. Star formation seems to have progressed along a southwest to northeast direction, from the diffuse H II region Sh2-88 A to the compact B1 and then to the UC region B2.

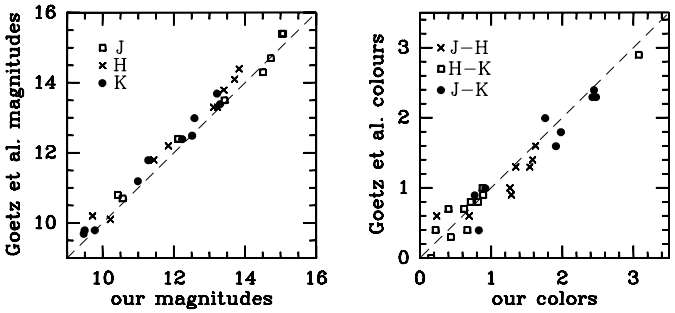

Fig. A.1. Comparison of the J, H, and K magnitudes, and of the $J-H$, $H-K$, and $J-K$ colors obtained by Goetz et al. (1999) and ourselves. The dotted lines are for equal values.

Appendix A: comparison with previous near-IR observations

Pipher et al. (1977) observed this region at 2.2 μm; their map shows a main emission peak with no optical counterpart, and two secondary peaks which they identified with two optically visible stars; they proposed these stars to be the exciting stars of the compact H II region Sh2-88B. Our near-IR study shows that their main emission peak corresponds (within 2″) to our star 82, which we identify as the main exciting star of the H II region B1, and that the secondary peaks are our stars 19 and 119, which we believe to be foreground stars – possibly associated with the complex, but not responsible for the ionization of the region.

A study of the extinction associated with Sh2-88B, based on JHK and Brγ photometry, has been presented by Goetz et al. (1999). Ten stars, identified in Table 1, are common to both their study and ours. Fig. A.1 compares the magnitudes and colors obtained. Our J, H, and K magnitudes are systematically lower than theirs, respectively by 0.23, 0.28, and 0.23 mag. The colors are not significantly different.

With regard to the systematic magnitude differences, it is difficult to know which study is in error; we can only stress that our calibration relies on six stars whereas we lack details about the Goetz et al. calibrations. In any case, this systematic difference is small, and does not modify the conclusions of Sect. 4.2. Goetz et al. (1999) do not comment about star 82, for which they give no J measurements. But their H and K measurements confirm our finding that star 82 is highly overluminous in K, by several magnitudes, for a main-sequence OB star (see Sect. 6.3).

Acknowledgements. We wish to thank G. Garay for providing us with high-resolution radio maps of the Sh2-88B region. Kieron Dean, while a student at Leeds University, and Frédéric Damour while a student at the Université de Provence, contributed to this study; we thank them for their work and enthusiasm. This research has made use of the Simbad astronomical database operated at CDS, Strasbourg, France.

References

Afflerbach A., Churchwell E., Accord J.M., Hofner P., Kurtz S., De Pree C.G., 1996, ApJS 106, 423
Allen C., Tapia M., Parrao L., 1977, Rev.Mex.Astron.Astrofis. 3, 119
Avedisova V.S., Kondratenko G.I., 1984, Nauchn. Inf. 56, 59
Beech M., Mitalas R., 1994, ApJS 95, 517
Bernasconi P.A., Maeder A., 1996, A&A 307, 829
Blair G.N., Peters W.L., Vanden Bout P.A., 1975, ApJ 200, L161
Blair G.N., Davies J.H., Dickinson D.F., 1978, ApJ 226, 435
Blitz L., Fich M., Stark A.A., 1982, ApJS 49, 183
Bonnell I.A., Davies M.B., 1998, MNRAS 295, 691
Bonnell I.A., Bate M.R., Zinnecker H., 1998, MNRAS 298, 93
Brand J., Blitz L., 1993, A&A 275, 67
Cesarsky C.J., Abergel A., Agnèse P., et al., 1996, A&A 315, L32
Chini R., Kreysa E., Mezger P.G., Gemünd H.-P., 1986, A&A 154, L8
Churchwell E., Walmsley C.M., Cesaroni R., 1990, A&AS 83, 119
Comoretto G., Palagi F., Cesaroni R., et al., 1990, A&AS 84, 179
Crampton D., Georgelin Y.M., Georgelin Y.P., 1978, A&A 66, 1
Deharveng L., Maucherat M., 1978, A&A 70, 19
Deharveng L., Caplan J., Lombard J., 1992, A&AS 94, 359
Deharveng L., Zavagno A., Nadeau D., Caplan J., Petit M., 1999, A&A 344, 943
Deharveng L., Peña M., Caplan J., Costero R., 2000, MNRAS 311, 329
Eiroa C., Casali M.M., Miranda L.F., Ortiz E., 1994, A&A 290, 599
Evans N.J., Blair G.N., Harvey P., et al., 1981, ApJ 250, 200
Felli M., Harten R.H., 1981, A&A 100, 42
Garay G., Rodriguez L.F., Moran J.M., Churchwell E., 1993, ApJ 418, 368
Garay G., Lizano S., Gomez Y., 1994, ApJ 429, 268
Garay G., Gomez Y., Lizano S., Brown R.L., 1998a, ApJ 501, 699
Garay G., Lizano S., Gomez Y., Brown R.L., 1998b, ApJ 501, 710
Goetz J., Pipher J., Forrest B., 1998, http://astro.pas. rochester.edu/∼jagoetz/S88B/Welcome.html
Goetz J., Howard E., Pipher J., Forrest B., 1999, http:// astro.pas.rochester.edu/∼jagoetz/S88B2/Welcome.html
Henkel C., Haschick A.D., Gusten R., 1986, A&A 165, 197
Heydari-Malayeri M., Testor G., Baudry A., Lafon G., de la Noë J., 1982, A&A 113, 118
Hiltner W.A., Iriarte B., 1955, ApJ 122, 185
Hodapp W.K., 1994, ApJS 94, 615
Jijina J., Adams F.C., 1996, ApJ 462, 874
Königl A., 1999, New Astronomy Reviews 43, 67
Léger A., Puget J.-L., 1984, A&A 137, L5
Lortet-Zuckerman M.C., 1974, A&A 30, 67
Mac Low M.-M., Van Buren D., Wood D.O.S., Churchwell E., 1991, ApJ 369, 395
Mathis J.S., 1990, ARA&A 28, 37
Monet D., Bird A., Canzian B., et al., 1998, USNO-A V2.0, A Catalogue of Astrometric Standards
Nadeau D., Murphy D.C., Doyon R., Rowlands N., 1994, PASP 106, 909
Ott S., Abergel A., Altieri B., et al., 1997, ASP Conf. Series 125, 34
Papoular R., 1999, A&A 346, 219
Pezzuto S., Strafella F., Lorenzetti D., 1997, ApJ 485, 290
Phillips J.P., Mampaso A., 1991, A&AS 88, 189
Pipher J.L., Sharpless S., Savedoff M.P., et al., 1977, A&A 59, 215
Pirogov L., Zinchenko I., Lapinov A., Myshenko V., Shulga V., 1995, A&AS 109., 333
Schaerer D., de Koter A., 1997, A&A 322, 598
Schmidt-Kaler T., 1982, in: Schaifers K., Voigt H.H. (eds.), Landolt-Bornstien (New Series) Group IV/ 2, Berlin: Springer-Verlag, 1
Simpson J.P., Rubin R.H., 1990, ApJ 354, 165
Stahler S.W., Palla F., Ho P.T.P., 2000, in: Mannings V., Boss A.P., Russell S.S. (eds.), Protostars and Planetary Systems IV, Tucson: University of Arizona Press, in press

Stark J.-L., Abergel A., Aussel H., et al., 1999, A&AS 134, 135
Stasińska G., Schaerer D., 1997, A&A 322, 615
Stetson P.B., 1987, PASP 99, 191
Testi L., Palla F., Natta A., 1999, A&A 342, 515
Vacca W.D., Garmany C.D., Shull J.M., 1996, ApJ 460, 914
Van Buren D., Mac Low M.-M., Wood D.O.S., Churchwell E., 1990, ApJ 353, 570
Weingartner J.C., Draine B.T., 1998, The universe as seen by ISO, in: Cox P., Kessler M.F. (eds.), ESA Publications Division, Noordwijk: ESTEC, p. 783
White G.J., Fridlund C.V.M., 1992, A&A 266, 452
Wouterloot J.G.A., Brand J., Fiegle K., 1993, A&AS 98, 589
Yorke H.W., Krugel E., 1977, A&A 54, 183
Yorke H.W., Welz A., 1996, A&A 315, 555
Zavagno A., Ducci V., 2000, A&A submitted
Zinchenko I., Henning T., Schreyer K., 1997, A&A 124, 385